New silica-based hybrid organic–inorganic solids containing oligoarylene-vinylene fluorophore-terminated phosphonates†

Céline Carbonneau, Richard Frantz, Jean-Olivier Durand,* Michel Granier, Gérard F. Lanneau* and Robert J. P. Corriu

Laboratoire de Chimie Moléculaire et Organisation du Solide (CNRS UMR 5637), Université Montpellier 2, case 007, Place Eugène Bataillon, 34095 Montpellier cedex 05, France. E-mail: durand@univ-montp2.fr, lanneaug@univ-montp2.fr; Fax: +33 4 67 14 38 52

Received (in Montpellier, France) 25th May 2001, Accepted 25th July 2001
First published as an Advance Article on the web 11th October 2001

Cogelation of new trimethoxysilane-derived oligoarylene-vinylene fluorophores terminated with diethyl and di-*tert*-butyl phosphonates is described. Materials were analyzed by solid state NMR techniques and BET. Fluorescence proves to be a very sensitive method to detect the chromophore and to obtain information about the organization inside the solid.

The syntheses and design of new highly functionalized materials have grown enormously in the last few decades, mainly because of the development of sol–gel chemistry.[1] This procedure is tolerant of a wide range of sensitive organic molecules, which lead to organic–inorganic hybrid solids combining the characteristics of the inorganic network and the properties of the functionalized organic moiety. Hybrid organic–inorganic solids based on a silica framework of general formula $x\mathrm{SiO_2}$, $\mathrm{O_{1.5}Si{-}R}$ have been studied in recent years, allowing the preparation of various sophisticated materials.[2] Application of organic–inorganic gels in the field of solids possessing optical properties is growing,[3] with potential applications such as non-linear optical devices,[3c–e] fluorescent pH probes,[3f] or fluorescent sensors for surface accessibility.[3g]

As phosphonates have proven to be useful building blocks in the generation of hybrid organic–inorganic materials,[4] preparation of silica-based materials possessing a covalently bonded phosphonate group functionality would be of great interest, to further investigate the reactivity and the coordination chemistry of the prepared phosphonate derivatives. Furthermore, phosphorus is a very sensitive NMR probe and ^{31}P solid state NMR could produce information about the behaviour of phosphonate groups inside the solid, concerning their local environments and their orientations (ordered or disordered). These materials would find use in potential applications such as ion detection,[5a] ion extraction, chromatographic devices,[5b] and syntheses of mixed oxides by grafting the phosphonate moiety on the surface of metal oxides.[6] However, very few syntheses of phosphonate-modified silicas have been published in the literature. Hovnanian and coworkers[7] have initially reported the parameters involved in the HF-catalyzed gelation of $\mathrm{(EtO)_3Si(CH_2)_2PO(OEt)_2}$ by using ^{29}Si and ^{31}P liquid and solid state NMR techniques. By reacting diethyl phosphonate functionalized chlorosilane on silica, Chevalier and colleagues[8] have described a modified silica for applications in $\mathrm{Ca^{2+}}$-sensitive field-effect transistors. Sullivan's recent publications[9] deal with the acid-catalyzed gelation of $\mathrm{(EtO)_3Si(CH_2)_2PO_3Et_2}$ and derivatives: solids were analyzed by solid state ^{13}C, ^{29}Si and ^{31}P NMR, and BET methods; hydrolysis of the diethyl phosphonate moiety was reported.

In connection with our work on luminescent solids, we describe here the nucleophilic gelation of new molecules[10] possessing a fluorescent carbon backbone covalently bonded to trimethoxysilane on one side and ethyl or *tert*-butyl phosphonate functionalities on the other. The gelation of the sensitive di-*tert*-butyl phosphonate ester functionality (readily cleaved in acid media[11]) has not been reported to our knowledge and is not compatible with an acid-catalyzed gelation procedure. The organic part was detected by fluorescence, even at very low proportions inside the solid. Luminescent properties of the materials thus prepared were analyzed, and produced information about the behaviour of the organic part inside the solid.

Results and discussion

Synthesis and analysis, including NMR

We have already described the syntheses of the precursors **1** and **2**[10] (Scheme 1) and their fluorescent behaviour in solution. Precursor **3** was synthesized by the Heck reaction of 4-styryltrimethoxysilane with diethyl 4-bromobenzylphosphonate in 90% yield (see ESI). The alkoxysilane moiety of the precursors **1–3** was reacted using a sol–gel procedure studied in our laboratory (Scheme 1). Solids with different proportions of chromophores were thus obtained (see ESI). Energy dispersive X-ray analysis (EDX) was used as a qualitative method to detect Si and P atoms. The technique showed that the samples were homogeneous on a micrometric scale, as no variation of the Si/P ratio was observed from one analysis to another on the same particle or on different particles. Quantitative analyses of the Si/P ratio were not performed. IR spectroscopy showed intense bands at 3200 (ν Si–OH), 1140–1050 (ν Si–O–Si) and 960 $\mathrm{cm^{-1}}$ (δ Si–O–C), which characterise the gel formation. The bands at 3023 (ν CH arom), 2980 (ν CH aliph), 1600, 1520 (ν C=C) and 1260 $\mathrm{cm^{-1}}$ (ν P=O) showed that the organic part was still present.

The CP MAS ^{29}Si NMR spectroscopy of gels **X1–X3** showed the classical T resonances ($\mathrm{SiO_3}$ units) for $x = 0$ and

---

† Electronic supplementary information (ESI) available: synthesis and analysis of **3**, conditions for the gelation of the precursors and characterization of the obtained xerogels, ^{29}Si CP MAS NMR spectra of **X2-0** and **X1b-5**. See http://www.rsc.org/suppdata/nj/b1/b104614b/

DOI: 10.1039/b104614b

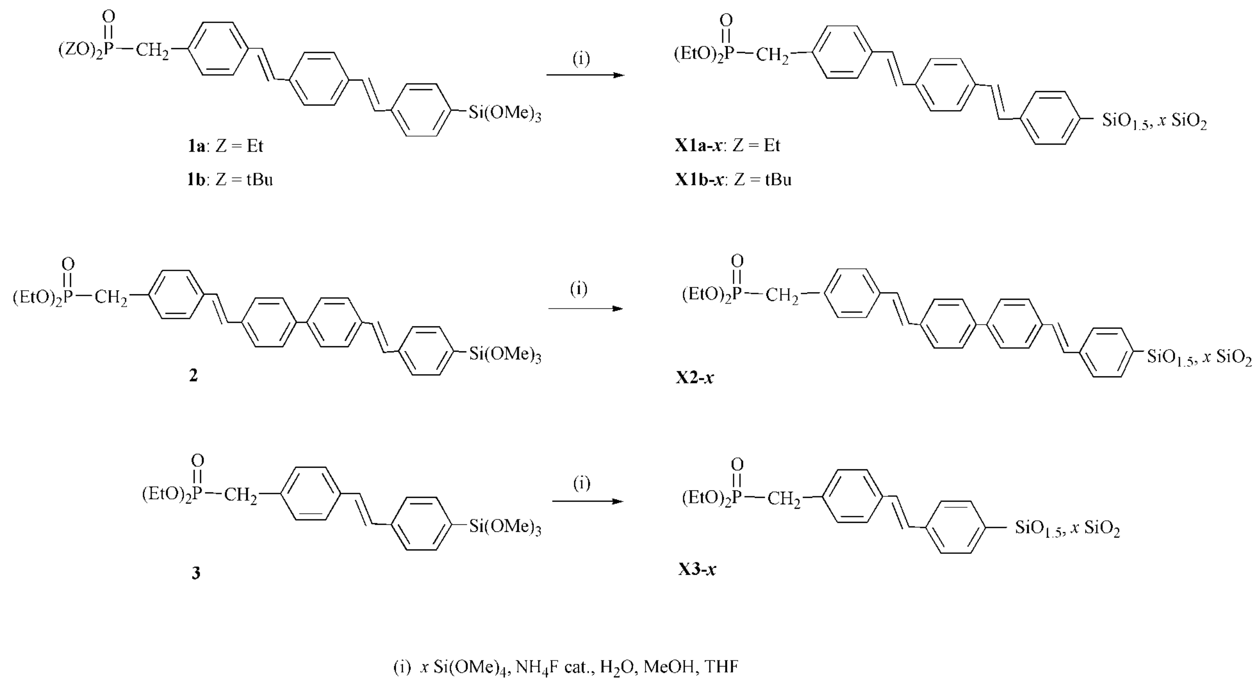

Scheme 1 Gelation of precursors **1**–**3**.

the T and Q resonances (SiO$_4$ units) for $x > 0$. The spectrum of **X2-0** (see ESI) showed a major T^3 resonance at -79 ppm attributed to SiO$_3$ groups possessing 3 siloxane bridges. The minor signal at -72 ppm corresponds to SiO$_3$ groups possessing 2 siloxane bridges. No Q signals were observed, which showed that no cleavage of the Si–C bond had occurred. The spectrum of **X1b-5** (see ESI) showed two major resonances at -109 (Q^4) and -101 ppm (Q^3), as well as a minor one at -92 ppm (Q^2); these correspond to SiO$_4$ units possessing 4, 3 and 2 siloxane bridges, respectively. The T^2 and T^3 resonances were observed at -72 and -78 ppm. The intensity of the Q resonance increased as x increased. These analyses were in agreement with well-condensed xerogels. CP MAS ^{13}C NMR analyses of xerogels **X1a**–**X3** (Fig. 1, top) showed resonances centred at 130–140 (aromatic and vinylic carbons), 62 (O=POCH$_2$) and 15 ppm (CH$_3$). Methoxy groups were not present ($x < 20$), indicating that total hydrolysis of the -Si(OMe)$_3$ units occurred. CP MAS ^{13}C NMR analyses of xerogels **X1b** showed resonances centred at 130–140 (aromatic and vinylic carbons), 81 (O=POC) and 30 ppm (CH$_3$) (Fig. 1, bottom).

These analyses showed that the carbon chain was not damaged during the sol–gel procedure. Note that the benzylic carbon (Ar–CH$_2$–PO$_3$) was hardly detected near 30 ppm, because of the high scalar coupling constant ($^1J = 150$ Hz) and the important dipolar coupling constant with phosphorus. HPDEC MAS ^{31}P NMR experiments showed only one signal at 27 ppm for xerogels **X1a–X3**. This value is in agreement with the ^{31}P chemical shift of the precursors **1–3**.[10] The symmetric signal indicates a macroscopic homogeneous environment of the phosphonates (Fig. 2, top). The peak width at half maximum is close to 5 ppm, which indicates that the phosphorus atom has different microenvironments in the disordered amorphous solid in contrast to crystalline well-ordered P-based materials, which show values of 0.8–1 ppm. Different contributions to the signal are thus involved and hydrogen bonds between phosphonates and silanol groups may also explain this broadening. No other signal was

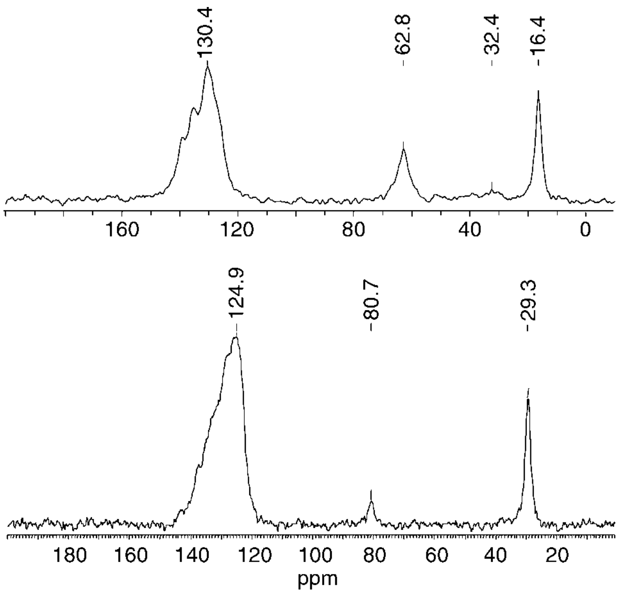

Fig. 1 ^{13}C CP MAS NMR (50 MHz) of xerogels **X3-2** (top) and **X1b-5** (bottom).

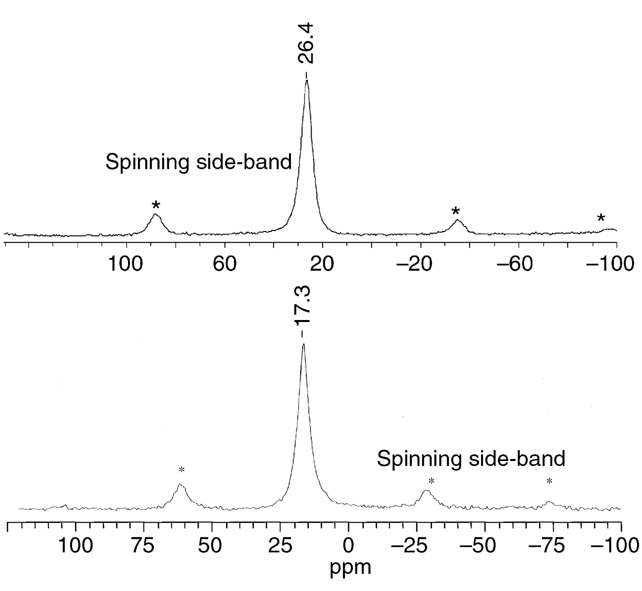

Fig. 2 ^{31}P HPDEC MAS NMR (80 MHz) of xerogels **X3-2** (top) and **X1b-10** (bottom).

detected, which showed that there was no hydrolysis or grafting by the phosphonate function.[11] Thus, the ethyl phosphonate moieties of compounds **X1a–X3** are stable in our mild sol–gel procedure. The ^{31}P signal of **X1b** was shifted to higher field, 18 ppm (Fig. 2, bottom). This chemical shift is in agreement with the value of the ^{31}P signal of the precursor **1b**.[10]

The di-*tert*-butyl ester was much more sensitive to acidic conditions and heat; cleavage of the ester began to occur after a few weeks at RT.[11]

We observed a gradual increase of the density of **X1–X3** upon increasing *x*, from 1.2 (**X3-0**) to 2.1 (**X1a-5000**, **X3-5000**). This is consistent with the density of a polysiloxane compound for $x = 0$ and the density of silica for $x = 5000$.

Nitrogen porosity measurement studies (BET)

Porosity measurements on samples **X1a–X3** were performed using N_2 sorption.[12] The results are presented in Table 1. We observed that the samples presented specific surface areas only for $x > 15$ and that specific surface area increased upon increasing *x*. We briefly studied the influence of *x* on the porosity of the xerogels **X1a–X3**. Representative adsorption–desorption isotherms for $x = 100$ and $x = 5000$ are presented in Fig. 3 and 4.

For xerogel **X2-100**, the adsorption–desorption isotherm was of type I, indicating that the solid was microporous (Fig. 3, middle). The characteristics of type I and type IV isotherms were observed for solids **X1a-100** and **X3-100**, indicating that the solids were micro- and mesoporous with a majority of mesopores (Fig. 3, top). For **X1a-100**, the hysteresis did not close, which suggests that some pores have an ink-bottle shape, with small pore openings that do not facilitate N_2 desorption. The microporous contribution to the texture of the solids is only important for **X2-100**. For a low proportion of the organic part in the solid ($x = 5000$), **X2-5000** presented an isotherm possessing the characteristics of type I and IV isotherms (Fig. 3, bottom). A micro- and mesoporous solid was thus obtained with a majority of mesopores (75%). **X1a-5000** and **X3-5000** presented isotherms of type IV indicating mesoporous solids (pore diameters of 40 Å) with a narrow distribution of pore diameters (Fig. 4). The contribution of micropores to the texture of the solids was very low. By decreasing the proportion of chromophores in the silica matrix, we observed an increase of the pore diameters and mesoporous solids were obtained. The precursor seems to contribute to the texture of the solid, as **X1a, X3** are different from **X2**, for the same value of *x*.

Luminescent studies

Xerogels **X1–X3** were first analyzed by solid state UV analysis. Representative absorption curves are presented in Fig. 5 after transformation by the Kubelka–Munk procedure. Maximum absorptions were not dependent on the proportion of chromophore inside the solids. Xerogels **X1a** presented two absorption maxima at 340 and 385 nm. For **X3**, when *x* varied from 2 to 10, a shoulder at 445 nm appeared (Fig. 5, bottom).

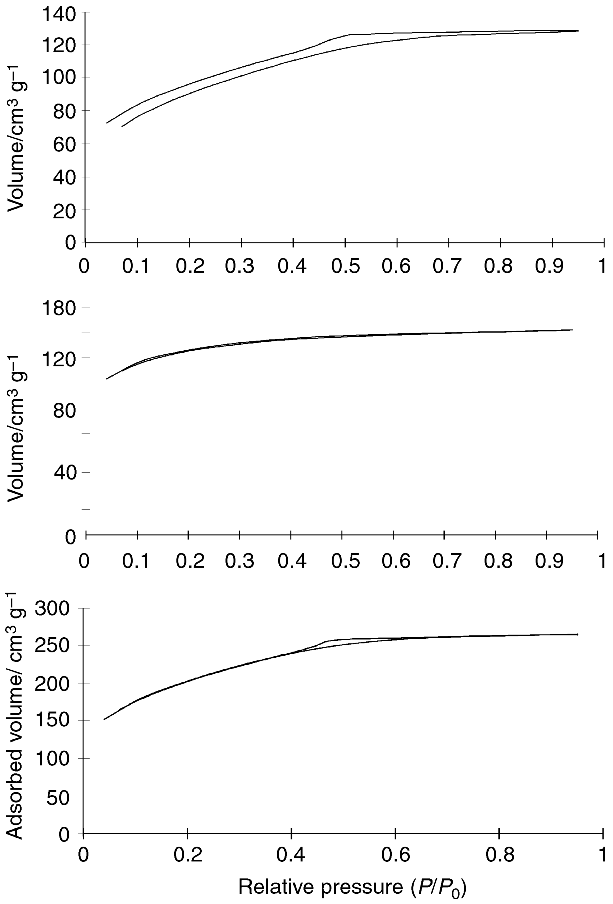

Fig. 3 Nitrogen adsorption–desorption isotherms for **X1a-100** (top), **X2-100** (middle) and **X2-5000** (bottom).

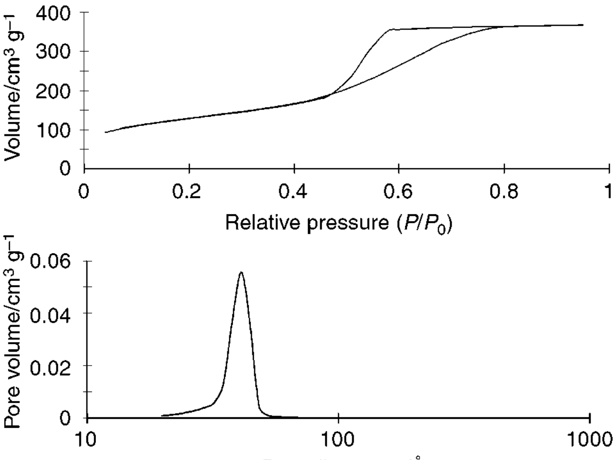

Fig. 4 Nitrogen adsorption-desorption isotherm and BJH pore size distribution for **X1a-5000**.

Table 1 Microporous contribution to the texture of the solid for $x = 100$, 5000

Xerogel	Isotherm type	Pore diameter/Å	Microporous volume (%)	Specific surface area/ $m^2\ g^{-1}$
X3-100	I and IV	10–50	8	451
X1a-100	I and IV	10–50	14	304
X2-100	I	10–40	66	509
X3-5000	IV	40	3	749
X1a-5000	IV	40	2.7	464
X2-5000	I and IV	10–40	25	725

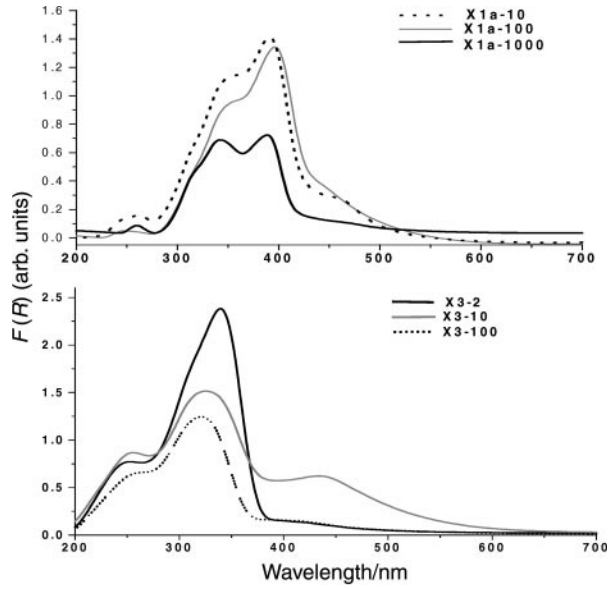

Fig. 5 Solid state UV analysis of xerogels **X1a** (top) and **X3** (bottom).

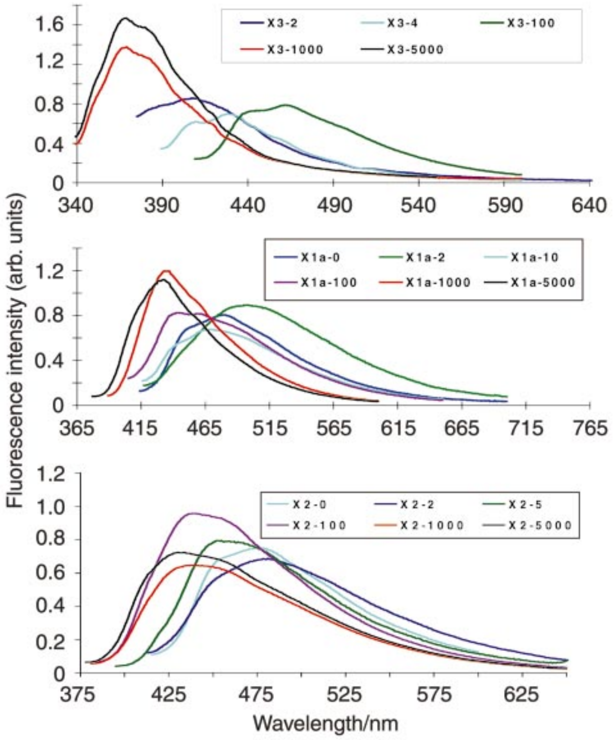

Fig. 6 Fluorescence spectra of xerogels **X3** (top), **X1a** (middle) and **X2** (bottom).

This could either be due to a new, more planar conformation of the chromophore or to the presence of ground state dimers or aggregates. After having determined the absorption region of the chromophores in the solids, we performed fluorescence spectroscopy. The excitation spectra did not depend on the emission wavelength and the emission spectra did not depend on the excitation wavelength, which suggests that only one species is involved in the fluorescence spectra. The excitation wavelength was fixed at the maximum of absorption determined by solid state UV analysis, at 320 nm for **X3**, 370 nm for **X2** and 365 nm for **X1a**.

Fluorescence was first used as a very sensitive detection method to characterize the presence of the chromophore. Indeed, NMR and IR solid-state techniques were not sensitive enough for the detection of the chromophore at low proportions inside the solid. The fluorescence technique allowed us to study the influence of the proportion of the organic part inside the silica ($x = 0$–5000) on the fluorescence emission spectra, in order to obtain information about the organization inside the solid. In contrast to the solid UV spectra, the fluorescence emission spectra were highly dependent on the proportion of chromophores for all the xerogels **X1-X3**, Fig. 6.

For xerogels **X3**, an important red shift of the $\lambda_{\max}$ emission ($\lambda_{\mathrm{m_{em}}}$) from 410 to 460 nm was observed when x was varied from 2 to 10. For $x = 10$ to 100, no significant shift of the $\lambda_{\mathrm{m_{em}}}$ at 460 nm was observed. For $x = 1000$ to 5000, an important blue shift to 360 nm was obtained. We have seen from BET experiments that the texture of our solids was different, when varying x from 2 to 5000. Thus, the matrix and interactions between the chromophore and matrix are different from one cogel to another and this could have an important effect on the conformation and behaviour of the chromophore in the solid. Our results could best be explained by the formation of different species of dimers (excimers) or aggregates in the ground state or the excited state at high concentrations ($x = 2$–100). Aggregates are known for stilbene and its derivatives: by layer deposition of PPV functionalized phosphonic acids on quartz substrate, Katz *et al.* obtained a red-shifted fluorescence emission.[13a] The red shift was explained by aggregation of aromatic compounds and exciton diffusion (an excitation initially produced on one molecule might hop to another molecule, generally by dipole–dipole-type interactions). Similar emission shifts have been observed in Langmuir–Blodgett films[13b] of stilbene and distyrylbenzene derivatives. Whitten[13c] has recently explained that different orientations of aggregates (J and H[13c]) of stilbene fatty acid derivatives in Langmuir–Blodgett films and supported multilayers were involved in the observed variation of the fluorescence. Levy and coworkers[14] have incorporated rhodamine (R6G) into silica gel through the sol–gel process. By increasing the concentration of rhodamine (R6G) adsorbed on the porous surface of sol–gels, they observed an important red shift of the fluorescence and referred to different orientations of J dimers at the silica surface to explain the red shift. In our case, at high proportions of chromophore in the gel, different kinds of aggregates could be involved when varying x from 2 to 100, with a variation of $\lambda_{\mathrm{m_{em}}}$ from 420 to 450 nm. The gradual decrease of the chromophore proportion should give rise to a distribution of aggregate geometries rather than to abrupt changes in the geometry. Each contributes to the fluorescence intensity, but the differentiation of these contributions within a distribution proves difficult.

At very low proportions of chromophore in the solid ($x = 1000$–5000), the texture of the solid becomes mesoporous. The chromophore trapped in the pores should be a monomer in the excited state because of reorientation and flexibility restrictions within a sol–gel matrix, which are not in favour of dimer formation.[15] Fox and colleagues[15c] have studied pyrene and pyrenyl-substituted trimethoxysilane to characterize films and glasses prepared by fast sol–gel hydrolysis. Chromophores were well dispersed with a rapid loss of excimer intensity, indicating that the chromophores were quickly isolated in the sol–gel matrix (low loading of pyrene derivatives). Note that the covalent attachment of the chromophore did not result in any change in the fluorescence emission. Thus, in our case, the important blue shift of 80 nm observed is attributed to the fluorescence of isolated chromophores for $x = 1000$–5000.

Xerogels **X1** and **X2** show the same type of behaviour as **X3** (red shift then blue shift when increasing x from 0 to 5000). But the red shift was less pronounced and appeared for $x = 0$ to 2. Then a progressive blue shift was obtained for $x = 5$ to 5000. As **3** is a shorter chromophore than **1** and **2**, this might explain the difference. Work is in progress with structurally closely related chromophores that give well-characterized excimers to obtain further information about orientations in the solid.

Conclusion

We have described the nucleophilic-catalyzed cogelation of trimethoxysilane-derived oligoarylene-vinylene fluorophore-terminated phosphonates. Analyses showed that the mild conditions of the procedure did not damage the fluorophore backbone and that the phosphonate environment was homogeneous. A low proportion of the organic part inside the solid is necessary to get high surface areas and mesoporous solids. Fluorescence spectroscopy proved a useful method for the detection of the chromophore at low levels and to give information about the behaviour of the organic part inside the solid. Work is in progress to get further information on this aspect. Further studies concerning the hydrolysis of ethyl and *tert*-butyl phosphonates and their coordination chemistry are also in progress and will be reported in due course.

Experimental

General methods

Manipulations of air-sensitive compounds were carried out under N_2. Solid state NMR spectra were recorded using Bruker 250 and 400 MHz spectrometers with an MAS 4 (spinning rate 9 KHz) or MAS 7 (spinning rate 3.5 KHz) probe. Surface area measurements (BET) were recorded using a Micromeritics Gemini III 2375 under nitrogen atmosphere. Fluorescence was registered on a SLM Aminco 8100 spectrometer, by reflection on a KBr pellet, scanning rate 2 nm s^{-1}. A front face sample holder was used and oriented at 60° in order to minimize the specular reflectance. Appropriate filters were used to eliminate Rayleigh and Raman scatters from the emission. IR data were obtained on a Perkin–Elmer 1600 FTIR spectrometer by transmission through a KBr pellet. Energy dispersive X-ray analyses were carried out with a Cambridge Stereoscan 360 electronic scanning microscope equipped with a Link AN 10 000 probe. Solid UV-visible spectra were collected on a Perkin–Elmer UV-vis spectrometer Lambda 14 and transformed using the Kubelka–Munk procedure. Barium sulfate was used as reference.

General protocol for the gelation of compounds 1–3

The precursor (**1**–**3**) was dissolved in a mixture of MeOH–THF (50 : 50). Then, x equivalents of tetramethoxysilane (TMOS) were added. The concentration in Si derivatives was 0.75 M for $x < 4$ and 0.5 M for $x > 4$. $(1.5 + 2x)$ mol of H_2O were added. Then, y% (y is the molar ratio calculated from the precursor) of 0.25 M NH_4F in water was added. After gelification (5–7 days), the gels were powdered, washed with MeOH, THF, acetone. Gels **X1a**–**X3** were dried at 120 °C under vacuum for 14 h. Gels **X1b** were dried under vacuum at RT for 12 h.

Acknowledgements

We thank V. Wintgens (Paris) and R. Lapouyade (Bordeaux) for helpful discussions concerning fluorescence spectroscopy.

References and notes

1 (*a*) C. J. Brinker and G. W. Scherer, *Sol-Gel Science: The Physics and Chemistry of Sol-Gel Processing*, Academic Press, San Diego, 1991; (*b*) L. L. Hench and J. K. West, *Chem. Rev.*, 1990, **90**, 33.

2 (*a*) R. J. P. Corriu and D. Leclercq, *Angew. Chem., Int. Ed. Engl.*, 1996, **35**, 1420; (*b*) R. J. P. Corriu, *Angew. Chem., Int. Ed.*, 2000, **39**, 1377; (*c*) U. Schubert, N. Hüsing and A. Lorenz, *Chem. Mater.*, 1995, **7**, 2010; (*d*) P. Judenstein and C. Sanchez, *J. Mater. Chem.*, 1996, **6**, 511; (*e*) R. H. Baney, M. Itoh, A. Sakakibara and T. Suzuki, *Chem. Rev.*, 1995, **95**, 1409; (*f*) J. Wen and G. L. Wilkes, *Chem. Mater.*, 1996, **8**, 1667; (*g*) E. Lindner, T. Schneller, F. Auer and H. A. Mayer, *Angew. Chem., Int. Ed.*, 1999, **38**, 2155.

3 (*a*) R. J. P. Corriu, P. Hesemann and G. F. Lanneau, *Chem. Commun.*, 1996, 1845; (*b*) J. P. Boilot, F. Chaput, J. Biteau, A. V. Véret-Lemarinier, J. P. Galaup, D. Riehl and Y. Lévy, *Ann. Phys. Fr.* (*Paris*), 1995, **20**, 727; (*c*) J. Biteau, F. Chaput, K. Lahlil, J. P. Boilot, G. M. Tsivgoulis, J. M. Lehn, B. Darracq, C. Marois and Y. Levy, *Chem. Mater.*, 1998, **10**, 1945; (*d*) J. P. Boilot, F. Chaput, T. Gacoin, L. Malier, M. Canva, A. Brun, Y. Levy and J. P. Galaup, *C. R. Acad. Sci., Ser. IIb*, 1996, **322**, 27; (*e*) B. Lebeau, S. Brasselet, J. Zyss and C. Sanchez, *Chem. Mater.*, 1997, **9**, 1012; (*f*) M. Ayadim, J. L. H. Jiwan, A. P. De Silva and J. P. Soumillion, *Tetrahedron Lett.*, 1996, **37**, 7039; (*g*) M. J. Bartels, M. Koeberg and J. W. Verhoeven, *Eur. J. Org. Chem.*, 1999, 2391.

4 (*a*) G. Alberti, in *Comprehensive Supramolecular Chemistry*, ed. J. M. Lehn, J. L. Atwood, J. E. D. Davies, D. D. MacNicol and F. Vögtle, Pergamon, Oxford, 1996, vol. 7, pp. 151–187; (*b*) F. Fredoueil, M. Evain, M. Bujoli-Doeuff and B. Bujoli, *Eur. J. Inorg. Chem.*, 1999, 1077.

5 (*a*) D. T. McQuade, A. E. Pullen and T. M. Swager, *Chem. Rev.*, 2000, **100**, 2537; (*b*) Y. R. Jin, L. Z. Zhang, S. J. Han, L. X. Zhang, J. M. Zhang, G. Q. Zhou and H. B. Dong, *J. Chromatogr., A*, 2000, **888**, 137.

6 G. Guerrero, P. H. Mutin and A. Vioux, *Chem. Mater.*, in press.

7 A. Cardenas, N. Hovnanian and M. Smaihi, *J. Appl. Polym. Sci.*, 1996, **60**, 2279.

8 Z. Elbhiri, Y. Chevalier, J. M. Chovelon and N. Jaffrezic-Renault, *Talanta*, 2000, **52**, 495.

9 (*a*) A. Aliev, D. L. Ou, B. Ormsby and A. C. Sullivan, *J. Mater. Chem.*, 2000, **10**, 2758; (*b*) M. Jurao-Gonzalez, D. L. Ou, B. Ormsby, A. C. Sullivan and J. R. H. Wilson, *Chem. Commun.*, 2001, 67.

10 C. Carbonneau, R. Frantz, J. O. Durand, G. F. Lanneau and R. J. P. Corriu, *Tetrahedron Lett.*, 1999, **40**, 5855.

11 Study of the hydrolyses of ethyl and *tert*-butyl phosphonates will be reported in due course. For a ^{31}P NMR study of the interactions of phosphonic acids with silica, see: I. Lukes, M. Borbaruah and L. D. Quin, *J. Am. Chem. Soc.*, 1994, **116**, 1737.

12 S. Brunauer, P. H. Emmett and E. Teller, *J. Am. Chem. Soc.*, 1938, **60**, 309.

13 (*a*) H. E. Katz, S. F. Bent, W. L. Wilson, M. L. Schilling and S. B. Ungashe, *J. Am. Chem. Soc.*, 1994, **116**, 6631; (*b*) W. F. Mooney, P. E. Brown, J. C. Russell, S. B. Costa, L. G. Pedersen and D. G. Whitten, *J. Am. Chem. Soc.*, 1984, **106**, 5659; (*c*) D. G. Whitten, *Acc. Chem. Res.*, 1993, **26**, 502.

14 F. Del Monte, J. D. Mackenzie and D. Levy, *Langmuir*, 2000, **16**, 7377.

15 (*a*) U. Narang and F. V. Bright, *Chem. Mater.*, 1996, **8**, 1410; (*b*) M. Ueda, H. B. Kim, T. Ikeda and K. Ichimura, *J. Mater. Chem.*, 1995, **5**, 889; (*c*) R. C. Chambers, Y. Haruvy and M. A. Fox, *Chem. Mater.*, 1994, **6**, 1351.